Macromolecular Research, Vol. 18, No. 2, pp 162-169 (2010)
DOI 10.1007/s13233-009-0138-4
www.springer.com/13233

PA6/MWNT Nanocomposites Fabricated Using Electrospun Nanofibers Containing MWNT

Byoung-Sun Lee and Woong-Ryeol Yu*

Research Institute of Advanced Materials(RIAM) and Department of Materials Science and Engineering, Seoul National University, Seoul 151-742, Korea

Received June 25, 2009; Revised September 7, 2009; Accepted September 9, 2009

Abstract: The electrospinning process with an applied electric field is used to extrude submicron fibers from polymeric solutions and has been recognized as a viable method for dispersing and aligning nanoparticles into a nanofibrous polymer matrix. In this study, electrospun nanofibers containing multi-walled carbon nanotubes (MWNTs) were used as a preform to fabricate MWNT reinforced polymer nanocomposites. The electrospun nanofibers were prepared by electrospinning a solution of polyamide 6 (PA6) and multiwalled carbon nanotubes (MWNTs). Raman spectroscopy, TGA, DSC, XRD, and TEM showed that the MWNTs were well dispersed and aligned in the electrospun nanofibers. The electrospun nanofibers in mat form were then consolidated into a solid composite by a thermal pressing. The initial modulus and tensile strength of the nanocomposites were improved by the reinforcement of the MWNTs. However, their breaking strain was lowered. This shortcoming was overcome by introducing a functional group onto the MWNTs through a surface treatment. Overall, the current method (modification of MWNTs, electrospinning, and thermal fabrication) can improve the tensile properties, including initial modulus, tensile strength and breaking strain, of PA6/MWNTs nanocomposites.

Keywords: carbon nanotubes, nanocomposites, electrospinning, nanofibers, mechanical properties.

Introduction

Carbon nanotubes (CNTs), which were discovered by Ijima[1] in 1991, consist of a rolled graphite sheet(s) with a hemi-sphere caps of fullerenes at both ends. Due to their rolled graphite structure, CNTs have superior in-plane properties, e.g., Young's modulus is 1 TPa and the resistivity is 50 μΩcm.[2] Many attempts have been made to employ these superior properties at the nano-scale to a macro-scale. Of these, composite applications for enhancing the mechanical properties of a polymer matrix have been studied extensively over the past decade. However, those applications have been tackled by the arrangement and adhesion of CNTs. Here, the arrangement refers to the dispersion and alignment of the CNTs in a polymer matrix. CNTs tend to entangle due to an interaction with each other and eventually aggregate. In addition, since CNTs are carbon allotropes and thus there are few functional groups for chemical bonding, strong interfacial adhesion of CNTs with other polymer molecules is a challenge.

A variety of methods have been reported to overcome the aggregation (entanglement) problems of nanoparticles, including optimal physical blending, *in-situ* polymerization, chemical functionalization and a variety of alignment methods.[3-16] However, electrospinning combined with the sonication process was chosen in this study. The electrospinning process involves two stages: the preparation and sonication of a polymer solution and its spinning by applying a high voltage in a syringe. Submicron sized fine fibers (nanofibers) are spun from the tip of the needle when the electric force overcomes the surface tension of the polymer solution. Here, the mechanical and electrical forces in the spinning process cause the CNTs to be dispersed and aligned in the nanofibers.[17]

A thermal processing was applied to the electrospun nanofibers in mat form to take advantage of dispersing CNTs in the nanofibers. The thermal processing was expected to increase the crystallinity and structural stability of the polymer matrix within the nanofibers, thereby enable the fabrication of polymer nanocomposites with well dispersed CNTs.

Because there are few functional groups on the CNTs for chemical bonding, the CNTs show poor interfacial adhesion with other polymer molecules. Therefore, the introduction of functional groups on the CNTs may be a key factor for improving the interfacial adhesion.[18-22] In this study, a diamine group was introduced to the CNTs. It is expected that through the surface treatments of CNTs, the nanocomposites fabricated from the electrospun nanofibers might enhance

*Corresponding Author. E-mail: woongryu@snu.ac.kr

the mechanical properties at a large deformation regime, such as the elongation strain, while the initial modulus and tensile strength may be improved due to the reinforcement effect of dispersed CNTs in the nanofibers. In summary, this study examined the validity of the electrospinning process for dispersing and aligning CNTs in a polymer matrix and whether this process can provide a means of fabricating polymer nanocomposites with enhanced mechanical properties.

Experimental

Materials. MWNTs (labeled diameter and length of 75 nm and 20 μm) were obtained from Nanokarbon Co., Ltd (Korea). Polyamide 6 (PA6) was chosen as the matrix material of the nanocomposites and was provided by Kolon. Co., Ltd (Korea). Sulfuric and nitric acid (H_2SO_4, 98% and HNO_3, 65% respectively), thionyl chloride ($SOCl_2$), tetrahydrofuran (THF) and ethylenediamine (EDA) (Samchun chemical Co., Ltd, Korea) were prepared for the surface modification of the MWNTs.

MWNTs Treatment. The diamine functional group was introduced onto the MWNTs using a procedure reported elsewhere.[19] Raw MWNTs (1 g) were dispersed in an acid mixture of sulfuric and nitric acid (3:1 by volume, 160 mL). The suspension was refluxed with constant stirring for 24 h at 65 °C and then sonicated for 1 h at room temperature (RT). The suspension was washed 5 times with distilled water and vacuum-filtered through a 0.2 μm millipore membrane. The filtered MWNTs were dried for 1 h at 100 °C in a vacuum drying oven. The acid treated MWNTs were suspended in 100 mL $SOCl_2$ with sonication for 1 h at RT. The suspension was vacuum-filtered and washed with anhydrous THF. The acid-treated MWNTs were dried in a vacuum oven for 1 h at RT. The modified MWNTs were suspended in excess EDA and refluxed for 12 h at RT. The MWNTs were then vacuum-filtered, washed 5 times with THF and dried in a vacuum oven at RT. The treated MWNTs are referred as AMWNTs.

Electrospinning and Composites Fabrication. Formic acid (Samchun chemical Co., Ltd, purity 99%) was used to make a solution of PA6 and MWNTs. The concentration of a solute mixture (PA6 and MWNTs) was fixed at 10 wt% in solution, and the concentration of MWNTs was varied: 0, 1, 2 and 3 wt% with respect to the solute mixture. The solutions were sonicated for 5 h to disperse the MWNTs before the electrospinning. Each solution was then electrospun under the following process conditions: voltage=20 kV, tip-to-collector distance = 8-12 cm, and the flow rate=0.5 mL/h. The nanofibers were collected in a random mat on a collecting drum. The nanofibrous mats were consolidated into solid nanocomposites by hot pressing at 240 °C, which is 20 °C higher than the $T_{m,\alpha}$ of the PA6. This hot pressing melts the polymer in the nanofibers, subsequently forming a continuous matrix phase in the nanocomposites.

Table I. MWNT Contents (wt%) in Spinning Solution and Nanofibers

Solution	1.0	2.0	3.0
Nanofibers	0.8	2.1	3.0

Characterizations. Thermogravimetric analysis (TGA) was performed for the electrospun nanofibers using TGA Q50 (TA instrument) to characterize the actual content of the MWNTs within them. The morphology of the nanofibers was observed by scanning electron microscope (SEM) using a high resolution instrument (JSM-6700F, Jeol). Transmission electron microscope (TEM) (JEM 1010, Jeol) was utilized to confirm that the MWNTs were embedded in the nanofibers and aligned along the nanofibers axis. Raman spectroscopy (T64000, Horiba) was employed to examine the geometric changes in the MWNTs within the nanofibers, focusing on the first order of the characteristic peaks of MWNTs (from 1200 cm^{-1} to 1700 cm^{-1}). Finally, differential scanning calorimetry (DSC) (Mettler Toledo) and X-ray diffraction (XRD) analysis were carried out to provide some information on the microstructure and crystallinity of the nanofibers. DSC and XRD scannings were carried out at a heating rate of 10 °C/min from 0 to 300 °C and 5°/min, respectively.

The effect of MWNTs on the mechanical properties of polymer nanocomposites was examined by performing tensile tests using an Instron-5543. The rate of extension was set to 10 mm/min. The fracture surface of the nanocomposites was observed by SEM. DSC and XRD analysis were also carried out under the same conditions as those for nanofibers. Fourier transform infrared spectroscopy (FTIR) was conducted using FT/IR 6300 (Jasco) to confirm the introduction of the diamine group onto the MWNTs.

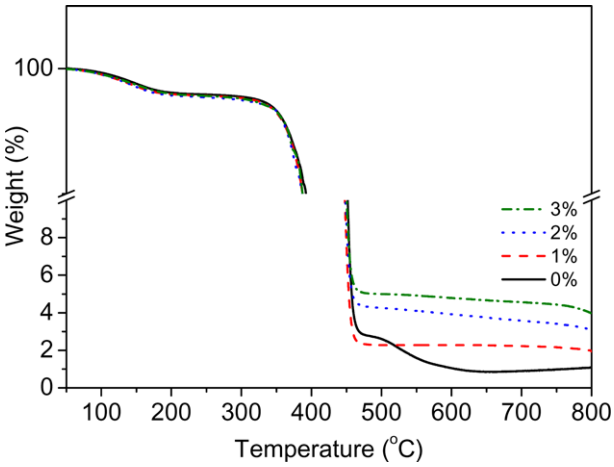

Figure 1. TGA thermogram of the PA6/MWNT composites.

Results and Discussion

Nanofibers: Dispersion and Alignment of MWNTs. The actual content of the MWNTs inside the nanofibers was determined using TGA (Table I and Figure 1). Residues of the nanofibers were analyzed at 600 °C because PA6 and MWNTs were decomposed at approximately 400 and 800 °C, respectively. As shown in, the contents of MWNTs were little changed, suggesting that the MWNTs in the polymer solution were successfully embedded into the nanofibers during the electrospinning process.

MWNTs used in this study were provided in entangled form in Figure 2(a) and their average diameter was observed as 62 nm (standard deviation: 19.25 nm). Note that MWNT modifies the spinnability of the polymer and thus the diameter distribution and morphology of the fibers was changed (Figure 3). Since the diameter of nanofibers appears similar to that of the MWNTs (Figure 2(b) and (c)), it can be deduced that each nanofiber accommodates only one MWNT along its axis if MWNTs are embedded in it, which can be confirmed by TEM observation. Figure 4 shows clearly this fact and also indicates that the nanofibers accommodating MWNTs became thick compared with neighboring nanofibers without MWNTs. On the other hand, since the nanofibers were produced in locally straightened form due to their

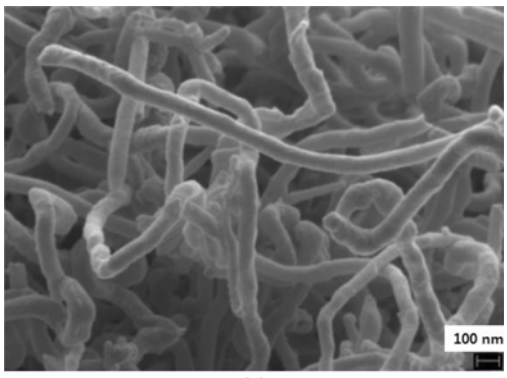

(a)

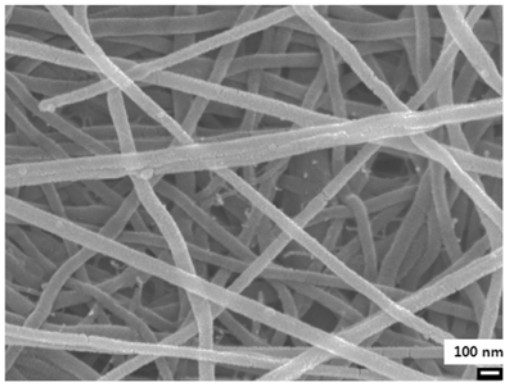

(b)

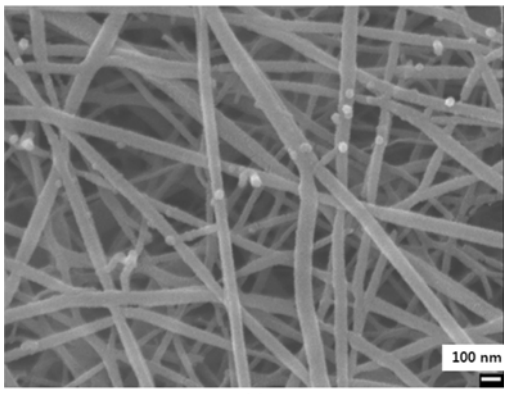

(c)

Figure 2. SEM photographs of (a) pure MWNTs, (b) and (c) nanofiber mats containing 0 and 2 wt% MWNT, respectively.

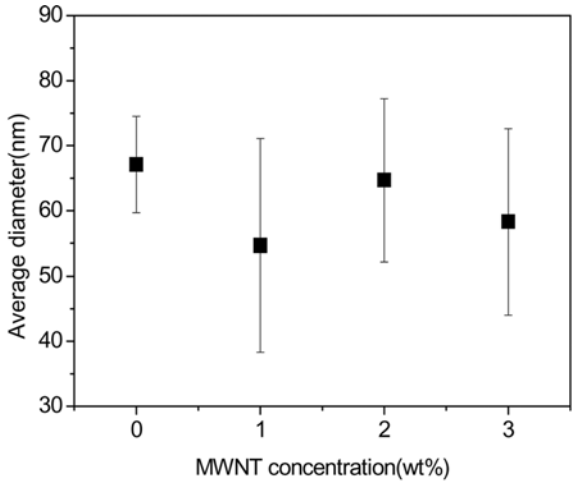

Figure 3. Average diameter of nanofibers with different MWNT concentrations.

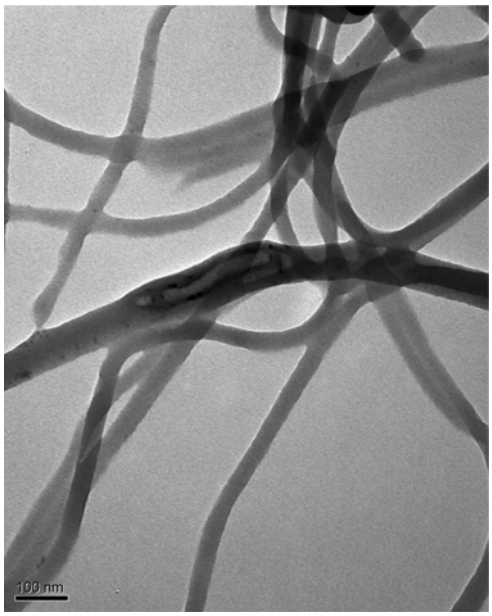

Figure 4. TEM photograph showing MWNTs embedded and aligned in the nanofibers.

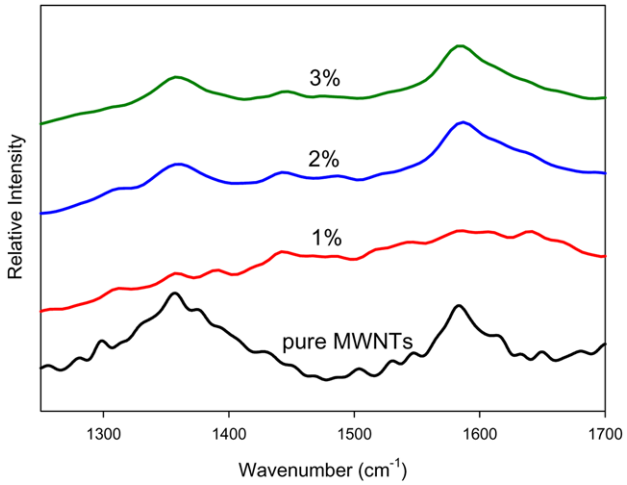

Figure 5. Comparison of the first order peaks of the Raman spectrum of raw MWNT and nanofibers containing MWNTs.

whipping tendency during the electrospinning process, MWNTs could be straightened and aligned along the fibers axis, which can be confirmed by Raman spectroscopy as follows.

The Raman spectra of the MWNTs and nanofibers were analyzed focusing on the first order of the two typical peaks at approximately 1365 cm^{-1} (D peak) and 1585 cm^{-1} (G peak), (Figure 5). The ratio of the two peak intensities (I_D/I_G) was decreased with increased MWNTs (Table II). This might be due to the alignment of the MWNTs in the nanofibers during the electrospinning. The D peak is related to the breaking of symmetry caused by the structural disorder, such as in-plane substitution heteroatoms, vacancies, grain boundaries, etc, while the G peak is relevant to the in-plane tangential stretch vibration mode (E_{2g}) of the graphite sheet.[23] The decrease in the ratio can be considered to be caused by a decrease in structural disorder, i.e., the MWNTs align along the nanofibers axis because the change of the peak intensity indicates some changes in geometry.

The microstructure of the matrix material in the composites is related to the composite properties involving the load transfer capability. Electrospinning may alter the microstructure of the PA6 polymer such as crystallinity. In this study, the microstructural change of PA6 nanofibers was investigated using XRD focusing on the effect of MWNTs on it. XRD profiles show two main peaks near 19.5° and 23° corresponding to (002/202) plane and (200) of PA6 α crystals, respectively (Figure 6(a)). Their downshift from the theoretical value[24] may be due to less close-packing during the electrospinning.[25] Figure 6(b) shows the crystallinity of the nanofibers with different MWNTs, which was obtained from the XRD analysis. The crystallinity of nanofibers increased with increasing the MWNTs contents. Since the same electrospinning condition was used for all samples, it can be concluded that MWNTs influenced the crystallization behavior of nanofibers, acting as a heterogeneous crystallization nuclei for PA6 polymer molecules during the electrospinning process.[26]

Table II. Comparison of the I_D/I_G Ratio of the MWNT and Nanofibers

Sample	Raw MWNT	1 wt% Nanofibers	2 wt% Nanofibers	3 wt% Nanofibers
I_D/I_G	1.17	0.91	0.91	0.91

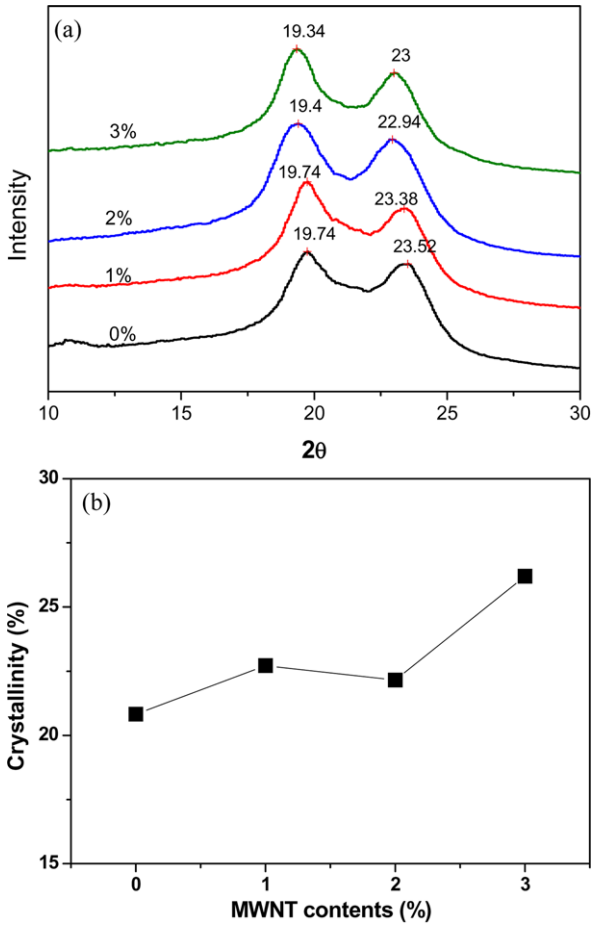

Figure 6. Microstructural change of nanofibers according to MWNTs. (a) XRD profiles and (b) crystallinity.

Nanocomposites: Mechanical Characterization. The tensile tests were carried out to examine the effect of the MWNTs on the mechanical properties of the PA6/MWNT nanocomposites. Figure 7 shows a typical stress-strain curve of the PA6 and PA6/MWNTs nanocomposites, showing that the initial stiffness and tensile strength were increased with increased MWNTs. However, the breaking strain was decreased significantly (see Figure 8 for a quantitative comparison of the mechanical properties). This can be explained by the MWNTs causing a stress concentration on the interfaces between the MWNTs and PA6 as the deformation proceeds, even though the MWNTs were well dispersed in the

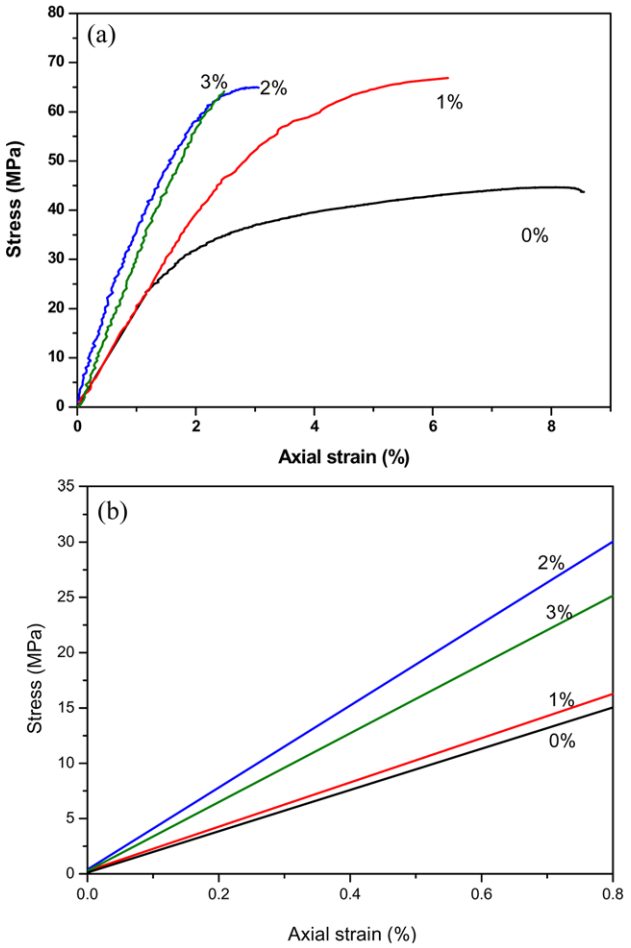

Figure 7. Typical stress-strain curves of the PA6/MWNTs nanocomposites: (a) total curves and (b) small deformation ranges.

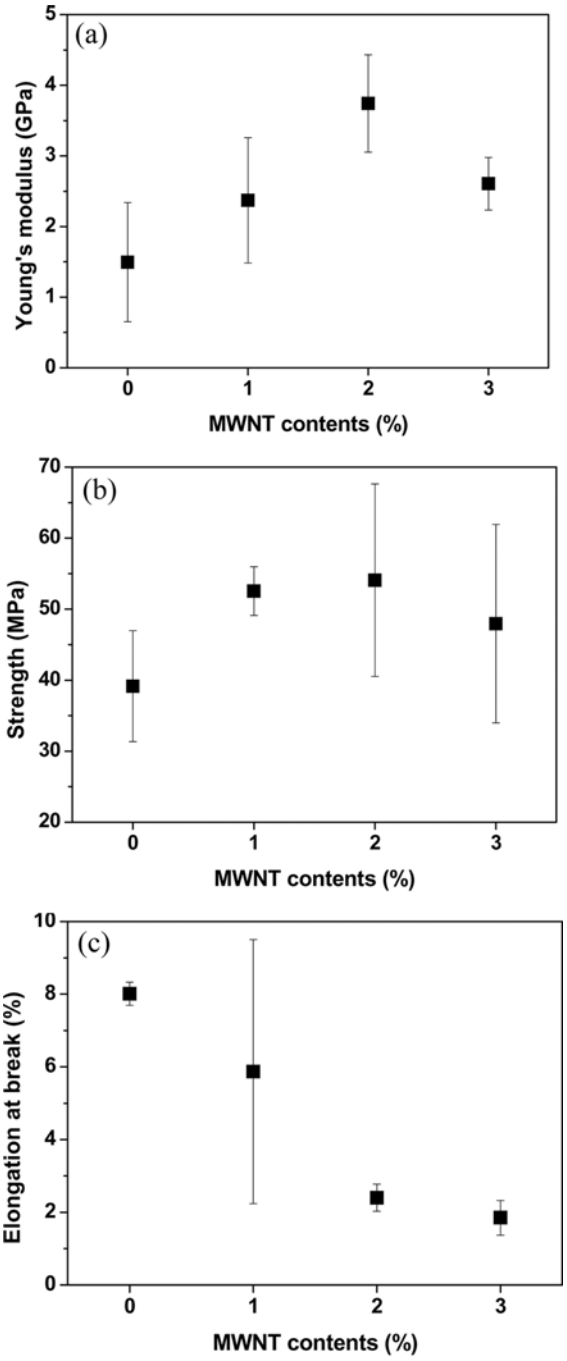

Figure 8. Mechanical properties of the PA/MWNT nanocomposites according to the MWNT contents: (a) initial modulus, (b) tensile strength, and (c) breaking strain.

matrix. This concentration of stress can be avoided or delayed by forming a chemical bond between MWNTs and PA6 molecules.

The microstructure of PA6/MWNT nanocomposites was again examined using XRD analysis (Figure 9). The first peak in the XRD profiles was shifted closely to the theoretical value, implying that the nanocomposites have more close-packing due to the heat treatment. The crystallinity was increased compared to the nanofibers, however, the effect of MWNTs on it was not clear in the nanocomposites, whereas MWNTs acted as neuclei in the nanofibers. To explain this fact, more investigations were carried out using DSC as follows.

There are two possible crystal structures, i.e., α (monoclinic) and γ (pseudo hexagonal) crystals, for PA6 polymer. These two crystals have different properties, e.g., their melting temperatures are different, e.g., 220 °C and 214 °C, respectively. While α crystal is a stable structure, γ crystal is metastable.[24] In the mechanical aspect, since the monoclinic structure is more difficult to slip than the pseudo-hexagonal structure, α crystal has higher strength and less breaking strain than γ crystal.[27] Figure 10(a) shows the DSC thermograms of nanofibers containing MWNTs, implying that some γ crystals were formed during the electrospinning because the melting peaks were shifted to the melting temperature of γ crystals. The DSC thermograms of nanocomposites (in Figure 10(b)) represent that the metastable γ crystals were

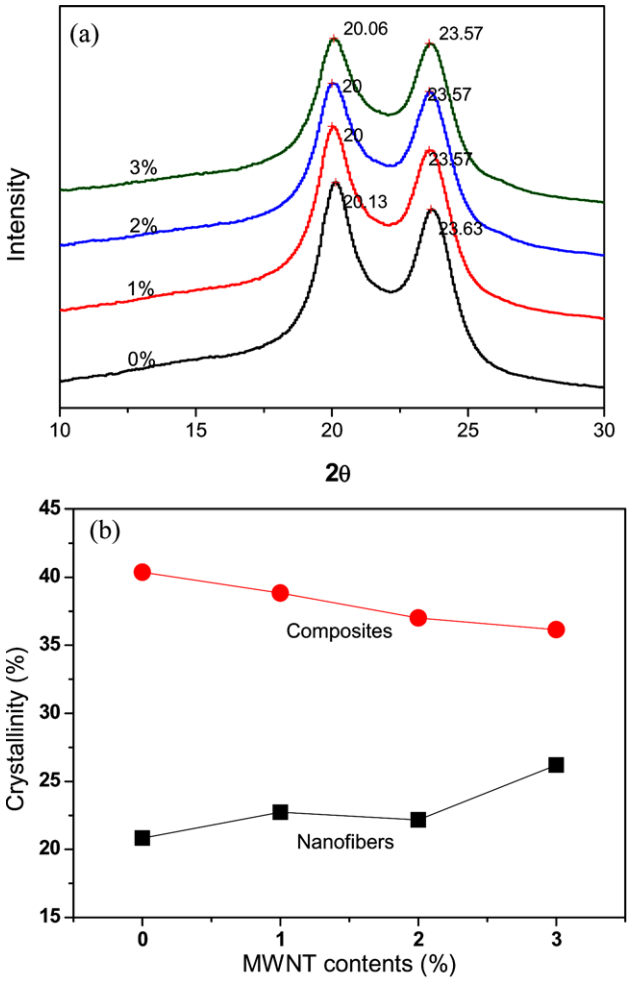

Figure 9. Microstructural change of nanocomposites according to MWNTs. (a) XRD profiles and (b) crystallinity.

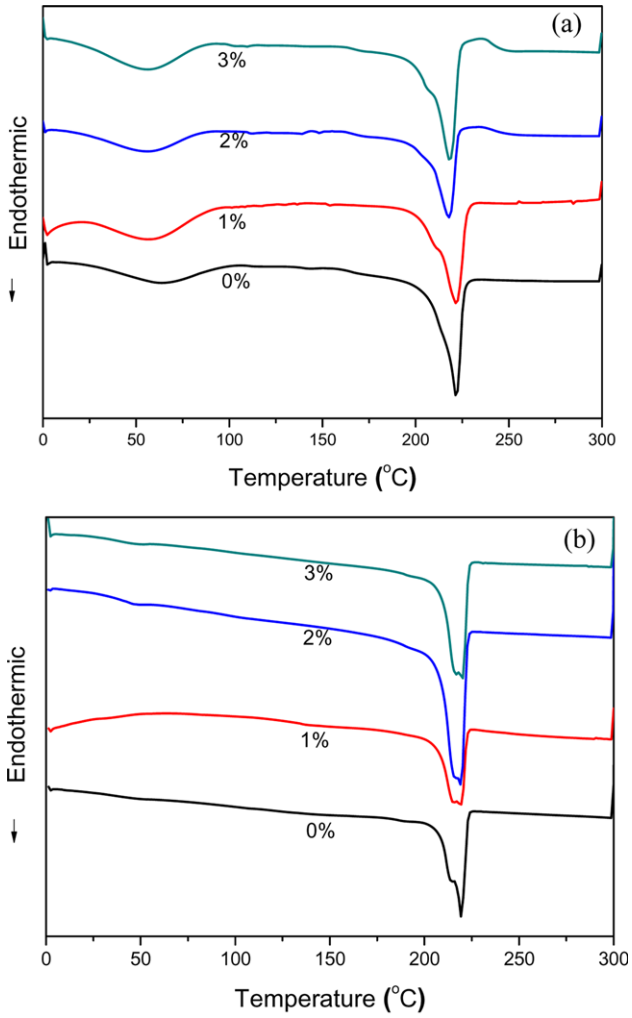

Figure 10. DSC thermograms of (a) nanofibers and (b) nanocomposites according to MWNT contents.

transformed into α crystal during the thermal treatment. This transformation may bring out slight decrease in the crystallinity of the nanocomposites.

Effect of Modified MWNTs on Nanocomposites. PA6/MWNT nanocomposites from the electrospun nanofibers showed a higher initial modulus and tensile strength due to the presence of dispersed MWNTs during the electrospinning. However, the breaking strain was not comparable to the neat PA6 polymer. This might be due to the weak bonding (Van der Waals bonding) between the MWNT and PA6 molecules, resulting in a concentration of stress at a relatively small deformation regime.

Recently, OH or NH group were introduced onto MWNT.[18-20] Both groups can produce hydrogen bonds with PA6 molecules. Diamine modified MWNTs were used in this study because the high electronegativity of an oxygen atom prefers OH-OH group bonding, which increased the likelihood of making aggregated carboxylic modified MWNTs[18] (see MWNTs treatment for detailed treatment). Diamine modified MWNT contain -$CONHCH_2CH_2NH_2$ groups,[19] which can be confirmed by FTIR analysis (see Figure 11 for the peaks at approximately 1480 and 1560 cm^{-1} belonging to the nitrogen based bonding: amine, amide, and imine).

A nanocomposite of PA6/AMWNT (1 wt%) was prepared using the same procedure, i.e., sonification, electrospinning and hot pressing, in order to investigate the effect of the AMWNTs on the mechanical properties of the nanocomposites. Figure 12 shows the stress-strain curves of the two nanocomposites with the neat PA6 polymer (see Figure 13 for a quantitative comparison of the mechanical properties). As mentioned previously, the initial modulus and tensile strength were improved by the effect of the AMWNT reinforcement in the matrix. Since both initial modulus and tensile strength depend on the MWNT loadings, they were not changed dramatically. However, the breaking strain was related directly to the interfacial bonding, and was improved significantly by attaching diamine groups to the

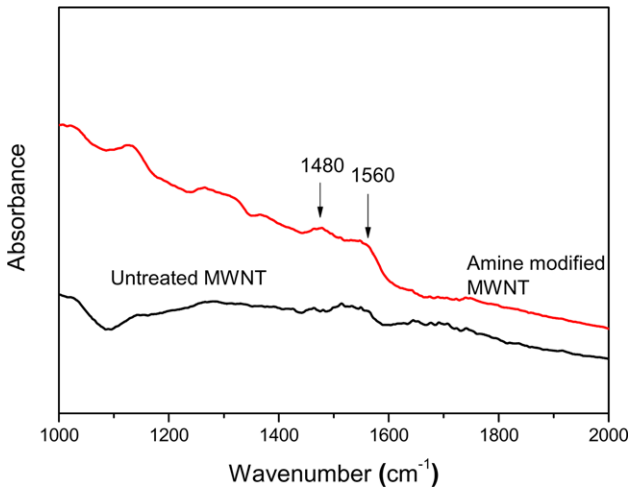

Figure 11. FTIR curves of the untreated and diamine modified MWNTs.

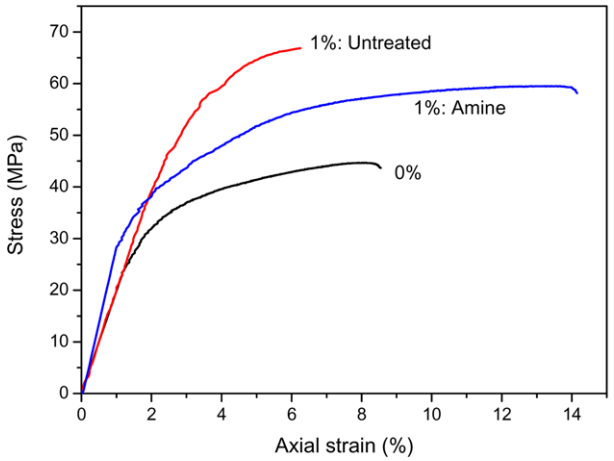

Figure 12. Comparison of stress-strain curves of PA6 polymer, PA6/MWNT nanocomposites with untreated MWNTs of 1 wt%, and PA6/MWNT nanocomposites with diamine modified MWNTs of 1 wt%.

MWNT. This fact can be confirmed observing the fracture surfaces of the nanocomposites in Figure 14. The fracture surfaces of nanocomposites with and without the MWNTs showed little pull-out debris. However, pull-out debris was observed in the nanocomposites containing the amine treated MWNTs due to the formation of hydrogen bonds between the MWNT and PA6, resulting in the increased breaking strain.

Conclusions

In this study, the electrospinning process and diamine modification of MWNTs were used to develop nanocomposites with a better initial modulus, tensile strength and breaking strain than the base polymer. The dispersion of MWNTs

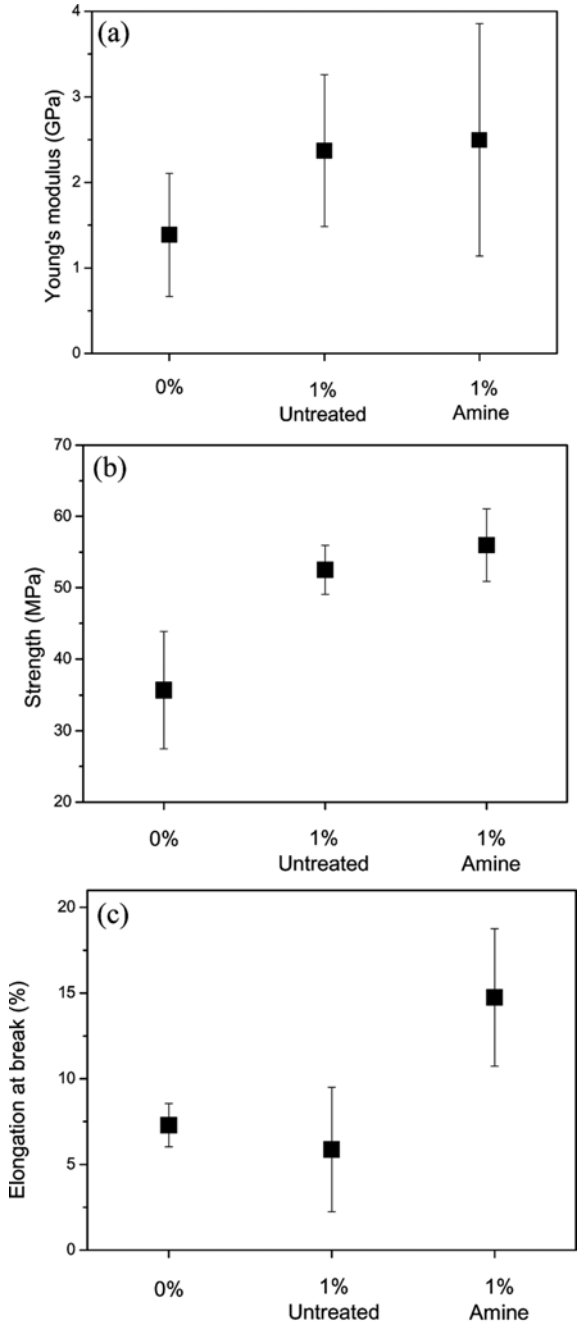

Figure 13. Mechanical properties of the nanocomposites according to the MWNT loading: (a) initial stiffness, (b) tensile strength, and (c) breaking strain.

into a polymer matrix was achieved through the sonication of a PA6/MWNT solution and subsequent electrospinning. The resulting nanofibers accommodated the MWNTs without aggregation problems due to the electrical and mechanical force applied by electrospinning process, which was confirmed by TEM and Raman spectroscopy. The consolidated nanocomposites from nanofibers showed improved initial modulus and tensile strength due to the reinforcement

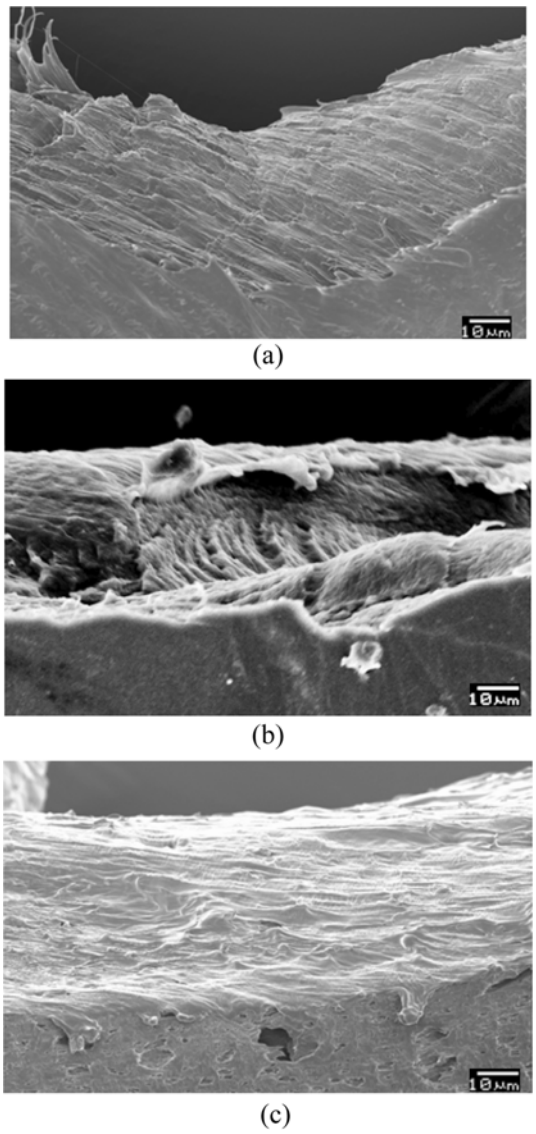

Figure 14. Fracture surface of the nanocomposites with (a) MWNT 0 wt%, (b) MWNT 1 wt%, and (c) AMWNT 1 wt%.

effect of the MWNTs. However, the breaking strain was reduced significantly. A functional group (diamine) was introduced into the MWNTs to solve this disadvantage. Finally, it was demonstrated that all tensile properties including initial modulus, tensile strength and breaking strain can be improved using the current method.

Acknowledgement. This study was funded by the Seoul R&BD Program and was also partially supported by DAPA and ADD, which the authors are grateful.

References

(1) S. Iijima, *Nature*, **354**, 56 (1991).
(2) H. S. Nalwa, Ed., *Handbook of nanostructured material and nanotechnology*, Academic Press, San Diego, 2000.
(3) X.-L. Xie, Y.-W. Mai, and X.-P. Zhou, *Mater. Sci. Eng. R,* **49**, 89 (2005).
(4) D. Qian, E. C. Dickey, R. Andrews, and T. Rantell, *Appl. Phys. Lett.*, **76**, 2868 (2000).
(5) J. Sandler, M. S. P. Shaffer, T. Prasse, W. Bauhofer, K. Schulte, and A. H. Windle, *Polymer*, **40**, 5967 (1999).
(6) X. Gong, J. Liu, S. Baskaran, R. D. Voise, and J. S. Young, *Chem. Mater.*, **12**, 1049 (2000).
(7) B. Z. Tang and H. Xu, *Macromolecules*, **32**, 2569 (1999).
(8) T. W. Ebbesen, P. M. Ajayan, H. Hiura, and K. Tanigaki, *Nature*, **367**, 519 (1994).
(9) H. Hiura, T. W. Ebbesen, and K. Tanigaki, *Adv. Mater.*, **7**, 275 (1995).
(10) W. Feng, X. D. Bai, Y. Q. Lian, J. Liang, X. G. Wang, and K. Yoshino, *Carbon*, **41**, 1551 (2003).
(11) Z. Jin, K. P. Pramoda, S. H. Goh, and G. Xu, *Mater. Res. Bull.*, **37**, 271 (2002).
(12) J. Fan, M. Wan, D. Zhu, B. Chang, Z. Pan, and S. Xie, *J. Appl. Polym. Sci.*, **74**, 2605 (1999).
(13) Y. Lin, B. Zhou, K. A. Shiral Fernando, P. Liu, L. F. Allard, and Y.-P. Sun, *Macromolecules*, **36**, 7199 (2003).
(14) J. E. Riggs, Z. Guo, D. L. Carroll, and Y.-P. Sun, *J. Am. Chem. Soc.*, **122**, 5879 (2000).
(15) T. Kimura, H. Ago, M. Tobita, S. Ohshima, M. Kyotani, and M. Yumura, *Adv. Mater.*, **14**, 1380 (2002).
(16) B. Vigolo, A. Penicaud, C. Coulon, C. Sauder, R. Pailler, C. Journet, P. Bernier, and P. Poulin, *Science*, **290**, 1331 (2000).
(17) P. Kannan, S. J. Eichhorn, and R. J. Young, *Nanotechnology*, **18**, 235707 (2007).
(18) J. S. Jeong, S. Y. Jeon, T. Y. Lee, J. H. Park, J. H. Shin, P. S. Alegaonkar, A. S. Berdinsky, and J. B. Yoo, *Diam. Relat. Mater.*, **15**, 1839 (2006).
(19) H. Meng, G. X. Sui, P. F. Fang, and R. Yang, *Polymer*, **49**, 610 (2008).
(20) G.-X. Chen, H.-S. Kim, B. H. Park, and J.-S. Yoon, *Polymer*, **47**, 4760 (2006).
(21) B. S. Kim, S. H. Bae, Y. H. Park, and J. H. Kim, *Macromol. Res.*, **15**, 357 (2007).
(22) I. Park, M. Park, J. Kim, H. Lee, and M. S. Lee, *Macromol. Res.*, **15**, 498 (2007).
(23) M. Burghard, *Surf. Sci. Rep.*, **58**, 1 (2005).
(24) T. D. Fornes and D. R. Paul, *Polymer*, **44**, 3945 (2003).
(25) J. S. Stephens, D. B. Chase, and J. F. Rabolt, *Macromolecules*, **37**, 877 (2004).
(26) C. Zhao, G. Hu, R. Justice, D. W. Schaefer, S. Zhang, M. Yang, and C. C. Han, *Polymer*, **46**, 5125 (2005).
(27) L. Penel-Pierron, R. Séguéla, J.-M. Lefebvre, V. Miri, C. Depecker, M. Jutigny, and J. Pabiot, *J. Polym. Sci. Part B: Polym. Phys.*, **39**, 1224 (2001).